Journal of Materials Chemistry A

Accepted Manuscript

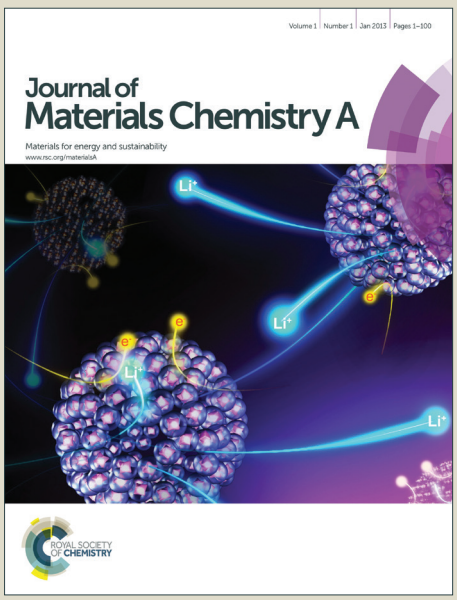

ROYAL SOCIETY OF CHEMISTRY

www.rsc.org/materialsA

Graphic Abstract

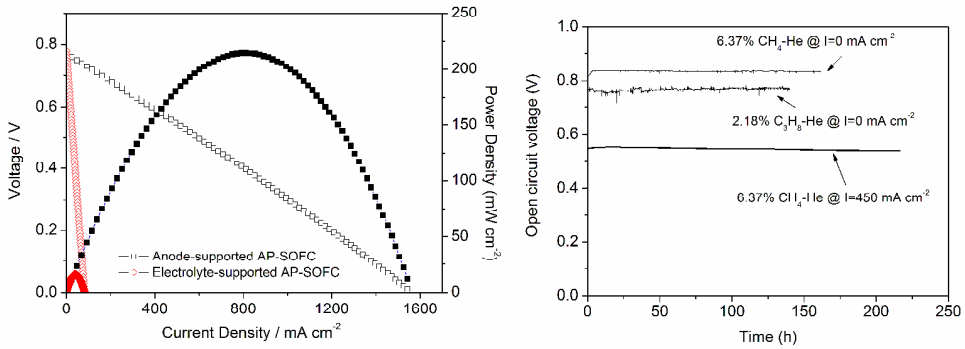

A long term operation stable, anode-supported AP-SOFC was developed to improve cell performance over 14 times without any coke formation.

Journal Name

RSCPublishing

ARTICLE

Coke free operation of an all porous solid oxide fuel cell (AP-SOFC) used as an O_2 supply device†

Cite this: DOI: 10.1039/xoxxoooooox

Y.M. Guo,[a,b] G. Largiller,[c] C. Guizard,[d] C. Tardivat[d] and D. Farrusseng*[a]

Received ooth January 2012,
Accepted ooth January 2012

DOI: 10.1039/xoxxoooooox

www.rsc.org/

Suppressing carbon deposition is crucial for operating solid oxide fuel cells (SOFCs) in dry hydrocarbon fuel. To prevent flammability and carbon deposition issues, a novel all porous SOFC (AP-SOFC) was developed as an O_2 supply device. In the present work, cell performances were studied using an anode-supported thin-film $Gd_{0.1}Ce_{0.9}O_{1.9}$ (CGO) configuration prepared by dry-pressing. The cell performance in a CH_4-He mixture was improved by over 14 times compared to an all porous electrolyte-supported SOFC. The peak power density of 183 mW cm^{-2} was obtained with 112 µm CGO porous electrolyte at 700°C. The long-term operation stability of the AP-SOFC was investigated with CH_4 and C_3H_8 under OCV conditions and with CH_4 under a constant current of 450 mA cm^{-2}. The anode-supported AP-SOFC was stable in CH_4 fuel for at least 10 days without observable coking of the anode. This indicates that the operation of an AP-SOFC in hydrocarbon fuels is a feasible process. An additional advantage of such a process is improved safety, due to the distribution of O_2 along the anode.

Introduction

Fuel flexibility is one of the significant advantages that solid oxide fuel cells (SOFCs) present over other types of fuel cells.[1, 2] The ability of SOFCs to run using hydrogen, a carbon-free fuel, is sometimes presented as an advantage, but the high cost of H_2 production, transportation and storage have limited the use of such systems, especially in mobile applications.[3] Therefore, the use of hydrocarbon fuel could simplify SOFC systems and improve their efficiency, which in turn could accelerate the commercialisation of SOFC systems for a variety of applications. Ni-based anodes are promising for SOFCs that use hydrocarbon as fuel, because nickel is an excellent catalyst for reforming both methane and higher hydrocarbons. Uncontrolled cracking leads, however, to rapid carbon deposition inside the SOFC anode, leading to catalyst coking and eventually deactivation.[3, 4] Various strategies have been adopted to accommodate Ni-based anodes for the use of hydrocarbon fuels while preventing carbon deposition: (a) introducing steam/O_2 reforming; (b) applying an electric current; (c) adding a nanocatalyst layer in the Ni-cermet support; and (d) inserting a dry reforming slab/buffer layer between the anode and the electrolyte.[5-8] While these strategies have been demonstrated to be effective on the laboratory scale, their scale-up to industrial applications remains a major challenge. For instance, steam reforming could provoke a strong temperature gradient in the cell that lowers cell performance while increasing mechanical stress.[9] Accordingly, it is necessary to develop a novel thermodynamics-based strategy that would allow the use of hydrocarbons as fuel on the Ni-cermet anode.

Compared to conventional dual chamber SOFCs (DC-SOFCs), single chamber SOFCs (SC-SOFCs), which are generally operated on a mixture of hydrocarbon fuels and air, have attracted much attention. In SC-SOFCs, the partial oxidation of hydrocarbon occurs first in the anode to produce a reformate mixture containing CO and H_2, which then reacts electrochemically with oxygen ions. The use of a hydrocarbon-air mixture in SC-SOFCs enables internal reforming over the Ni-based anode catalyst without addition of steam, because carbon deposition can be controlled by adjusting the oxygen content in the fuel-air mixture.[10] The risk of explosion related to working with fuel-air gas mixtures is, however, a major drawback of SC-SOFCs. For example, the methane-to-oxygen ratio (R_{mix}) has to be larger than 1.07 to prevent flammability issues.[11] Unfortunately, this limitation of flammability results in low fuel utilisation. Furthermore, it is acknowledged that high

[a] Institut de Recherches sur la Catalyse et l'Environnement de Lyon (IRCELYON), University Lyon 1, CNRS; 2, avenue Albert Einstein, 69626 Villeurbanne, France.
E-mail : youminguo@126.com; david.farrusseng@ircelyon.univ-lyon1.fr.
[b] School of Physics and Materials Science, Anhui University, Hefei 230601, P.R. China
[c] CEA, LITEN/DTNM/SERE, Laboratoire Recyclage et Valorisation des Matériaux ; 17 avenue des Martyrs, 38000 Grenoble, France.
[d] Laboratoire de Synthèse et Fonctionnalisations des Céramiques, UMR 3080 CNRS/Saint-Gobain, 84306 Cavaillon, France.
†Electronic Supplementary Information (ESI) available: See DOI: 10.1039/b000000x/

fuel efficiency and high power output cannot be obtained simultaneously in SC-SOFCs due to flammability and flow pattern issues.[12]

Very recently, we proposed a novel all porous SOFC (AP-SOFC) configuration consisting of three porous layers of anode, electrolyte and cathode, respectively, which are separated into two chambers. This AP-SOFC is allowed to control the distribution of gaseous O_2 at the anode side, thus preventing the deactivation of the anode and generating heat by auto-thermal reforming.[13] The oxygen distribution in the anode is controlled by the porosity of a $Gd_{0.1}Ce_{0.9}O_{1.9}$ (CGO) electrolyte and differential pressure (ΔP) applied between the cathode and the anode. In this AP-SOFC, the oxidative reforming of hydrocarbons consequently operates in a similar fashion to SC-SOFCs, but within a safer and better controlled process.[14-16] Our first attempt dealt with an electrolyte-supported AP-SOFC with a thick CGO porous electrolyte (2 mm). The peak power density reached only 15 mW cm^{-2} with methane as fuel and air as oxidant, because of the large ohmic resistance resulting from the thick porous electrolyte.

It is recognized that reducing the thickness of the electrolyte could increase the maximum power density of an anode-supported SOFC.[17] SOFCs based on dense thin-film doped CeO_2 electrolytes have already been tested and have exhibited excellent electrochemical performances.[18-20] In one example, the cell performance was improved from ~200 mW cm^{-2} to ~630 mW cm^{-2} by reducing the thickness of the CGO electrolyte from 75 μm to 16 μm.[17] Because the thin electrolyte can no longer be the component that provides mechanical support, one of the porous electrodes must take over this function. State-of-the-art SOFCs therefore use anode materials as supporting layers. Several approaches have been reported regarding the fabrication of the thin-film electrolyte, in which dry-pressing is proposed as a simple, reproducible and very cost effective technology.[18, 19]

Herein, we present for the first time an anode-supported all porous SOFC that contains thin-film CGO electrolyte prepared via dry-pressing. This new AP-SOFC has a power density of 214 mW cm^{-2} at 750°C, which is over 14 times that observed with an electrolyte-supported configuration. It can operate for at least 220 hours under dry methane and dry propane without coke formation.

Experimental

Fuel cell fabrication

The electrolyte, anode and cathode powders used in this study were of commercial origin. The CGO electrolyte powder (Marion Technologies) was mixed with Sigmacell Cellulose Type 20 (Sigma-Aldrich) by ball-milling. For the fabrication of the anode-supported AP-SOFC, a dual dry-pressing technique was adopted. Well-mixed anode materials, composed of the proper amounts of NiO, CGO and pore former, were prepared by ball-milling in alcohol liquid medium for 1 h. After drying, the anode powder was pressed into a disk-shape substrate with a 30 mm stainless steel die at 100 MPa, and then the proper amount of mixed CGO powder was distributed homogeneously over the surface of the anode substrate remaining inside the die. After co-pressing at a pressure of 250 MPa, a dual layer of anode substrate and thin-film electrolyte was sintered at 1400 °C for 5 h. The cathode layer was prepared by spray-coating. The powders, $Ba_{0.5}Sr0_{.5}Co_{0.8}Fe_{0.2}O_{3-\delta}$ (BSCF, Marion Technologies, France) and CGO (BSCF/CGO=70/30 by weight) for the cathode, were mixed with ethylene glycol, isopropanol and glycerine to obtain a slurry of the desired viscosity. The ink obtained was sprayed onto the CGO electrolyte surface and then co-fired at 1000 ℃ for 2 h. Finally, diluted gold paste (Fuel cell materials), used as a current collector, was painted onto the surface of the cathode, followed by sintering at 800 °C for 2 h.

Characterisation

The obtained fuel cell samples were sealed in the reactor using Au O-rings under mechanical pressure. Prior to the fuel cell test, the N_2 permeation through the AP-SOFC single cell was measured at 700 °C. For this test, pure N_2 was fed at the cathode side, He was used at the cathode chamber under atmospheric pressure. The differential pressure between the cathode and the anode ($\Delta P=P_{cathode}-P_{anode}$, bar) was varied by adjusting the pressure at the cathode by closing the valve of the outlet in a stepwise fashion, while maintaining 1 bar pressure at the anode chamber. The flow rate of gas in the anode was measured by a flow meter (Bis20 digital). Similarly, O_2 permeation measurements were carried out by switching the gas in the cathode from N_2 to air. The O_2 concentration in the anode chamber was analysed by an online gas chromatograph (micro GC, SRA instruments).

For the fuel cell test, a fuel mixture composed of He and dry hydrocarbon (CH_4 or C_3H_8) was fed at the anode side, and air, serving as the oxidant, was fed at the cathode (total flow rate of 200 ml min^{-1}). The ΔP between the cathode and the anode was controlled as the N_2 permeation test. *I-V* polarisation curves were collected using a Bio-Logic potentiostat/ galvanostat (EPP-400/4000) with EC-Lab software. The electrochemical impedance measurements were carried out on a Solartron 1260A frequency analyser with AC amplitude of 200 mV under open circuit conditions from 10^5 to 0.1 Hz.

In this study, the microstructures of the AP-SOFC tested were examined using a scanning electron microscope (SEM, ZEISS EVO HD-15). The elemental distributions in the anode layer after testing were analysed by SEM equipped with an energy dispersive X-ray analyser (EDX).

Results and discussion

Microstructural characterisation

The scanning electron microscopy (SEM) micrograph of the AP-SOFC structure of Ni+CGO anode | CGO porous electrolyte | $Ba_{0.5}Sr_{0.5}Co_{0.8}Fe_{0.2}O_{3-\delta}$ (BSCF) + CGO cathode (after test) is shown in Figure 1. The single cell had the desired porous architecture. The thickness of porous CGO was 112 μm. We can see that both the Ni+CGO anode and the BSCF+CGO

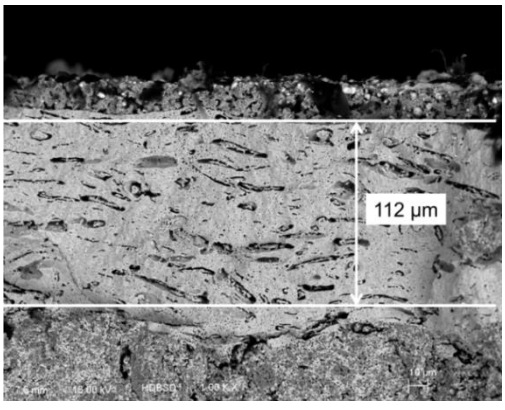

Fig. 1 SEM micrograph of the cross-section of the AP-SOFC after testing, showing the three porous layers: BSCF-based cathode (top), porous CGO (centre) and Ni-based anode (bottom).

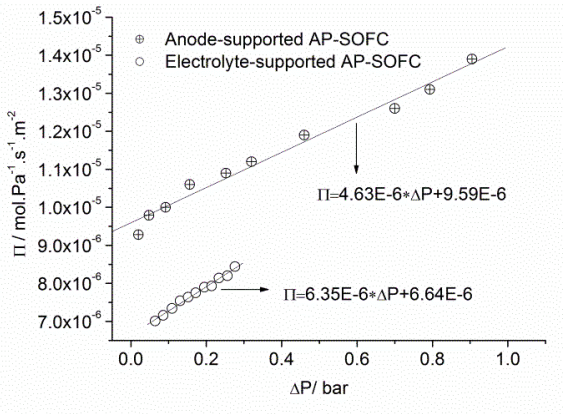

Fig. 2 Mass transport characterisation by N_2 permeation of the anode-supported AP-SOFC as a function of differential pressure at 700°C. The data for electrolyte-supported AP-SOFC can be found in [ref. 13].

cathode were highly porous. It is important to note that the interfaces of the three cell components were very well-integrated with no tendency to peel off, meeting the first prerequisite for promising cell performance.

Gas permeation test on a single cell

Prior to the fuel cell performance tests, the gas transport characteristics of the AP-SOFC were characterised. Figure 2 shows the nitrogen permeation as a function of ΔP applied between the cathode and the anode at 700°C. As with an electrolyte-supported AP-SOFC, the mass transport regime in the gas phase was also dominated by Knudsen flow, especially at lower ΔP (Table S1 in the ESI).[13] For example, Knudsen flow accounted for more than 90% at ΔP=0.1 bar.

Air permeation was also measured (Fig. S1). The O_2 concentration increased linearly with ΔP. When ΔP was 0.9 bar, the O_2 concentration at the anode side reached 3.1%. Thus, the AP-SOFC plays the role of an oxygen supply device that can be controlled by adjusting the pressure at the air side (ΔP).

Single cell testing

According to the Nernst equation, the OCV depends on the difference in the partial pressure of oxygen between the cathode and the anode. Therefore, the OCVs were measured under 6.4% CH_4-He as a function of ΔP (Figure 3a). The resulting volcano plot shows a maximum value of 0.831 V at turning point ΔP (ΔP_{TP}) = 0.40 bar. This is consistent with our previous result for an electrolyte-supported AP-SOFC and with simulations based on the Nernst equation.[13] When ΔP was lower than ΔP_{TP}, the OCV slightly increased with ΔP; this can be attributed to the slight increase of the partial pressure of O_2 at the cathode side. Meanwhile, at the anode side, the gaseous O_2 diffusing through the CGO thin-film reacted with hydrocarbon to form CO and H_2, resulting in a small trace of oxygen at the anode. When ΔP was higher than ΔP_{TP}, the OCV decreased with increasing ΔP, which can be attributed to the evolution of R_{mix}. Moreover, with a further increase of ΔP, the gaseous O_2 flux increased from the cathode to the anode side, leading to lower R_{mix} in the anode

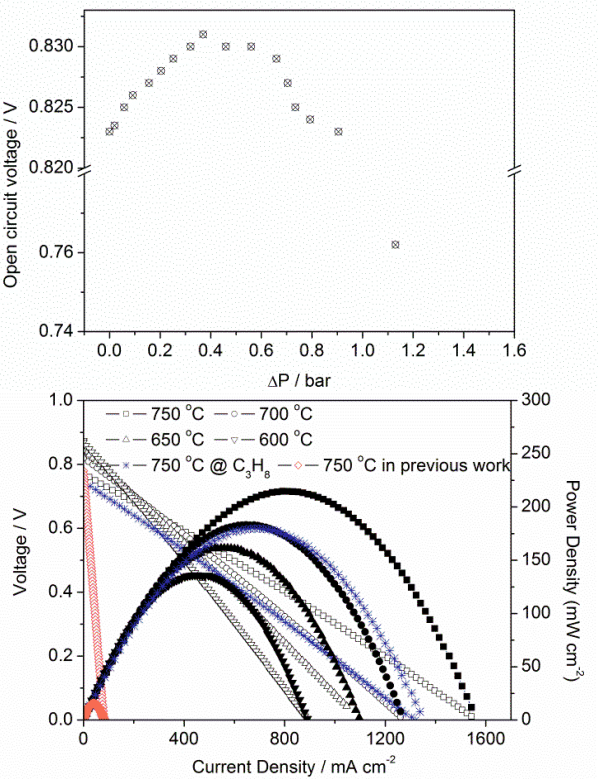

Fig. 3 (a) OCVs of the electrolyte-supported AP-SOFC as a function of the differential pressure at 700°C; (b) Comparison of fuel cell performances between electrolyte- and anode-supported AP-SOFCs under 6.4% CH_4-He/Air atmosphere at various temperatures. The data for electrolyte-supported AP-SOFC can be found in [ref. 13].

side, in agreement with thermodynamic data.[21] Electrochemical performance tests were carried out with ΔP = 0.40 bar, which corresponds to the highest OCV. The current-voltage behaviour of AP-SOFCs operating in 6.4% CH_4-He at various temperatures is shown in Figure 3b. The OCVs obtained in this study (0.78-0.94 V) were high, considering that O_2 was present in the anode chamber. Although the reduction of Ce^{4+} to Ce^{3+} may occur at the very surface of the grains, the thermodynamic conditions are not favorable for a reduction of the bulk to Ce^{3+}. In this study, as shown by Fig. S1, the oxygen partial pressure in the ceria oxide is relatively high (>0,2 atm), which should avoid the reduction of ceria in the bulk..[21, 22] Under dry CH_4, our AP-SOFC achieved peak power densities (PPD) of 214, 183, 161 and 135 mW cm^{-2} at 750, 700, 650 and 600 °C, respectively. The peak power density at 750 °C was over 14 times that obtained for the electrolyte-supported AP-SOFC in CH_4 fuel (insert data in Figure 3b), which is a major improvement in performance. Also the temperature at the surface of the anode should be increased by heat generation of the oxidation reactions, we did not oberve a siginicant temperature shift when the methane is feed. This can be explained by the relatively low methane partial pressure.

The C_3H_8 concentration was fixed at 2.1% to provide a constant O/C ratio with respect to CH_4. The OCV of 0.75 V and the PPD in 2.1% C_3H_8 was 179 mW cm^{-2} at 750°C (Figure 3b), demonstrating that this AP-SOFC can feasibly be used with higher hydrocarbon fuels, which are known to provoke severe coking. The difference of performances

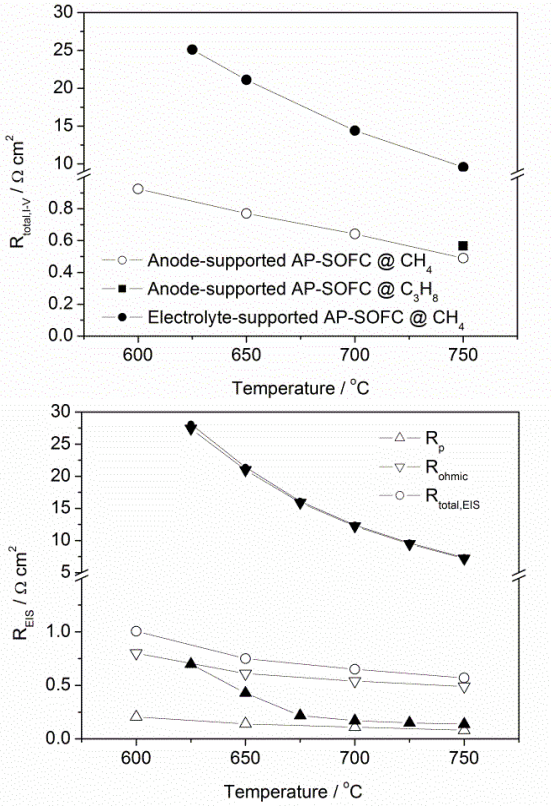

Fig. 4 (a) Total area-specific resistance of both electrolyte- and anode-supported AP-SOFCs calculated by I-V curves as a function of temperature; (b) Comparison of different resistances for AP-SOFCs operating in CH_4 calculated by EIS as a function of temperature: (open symbols) anode-supported AP-SOFC; (solid symbols) electrolyte-supported AP-SOFC.

between CH_4 and C_3H_8 may arise from various factors (activation of the hydrocarbon, activation energy, different reduction of the ceria...), which can be hardly unraveled.

The total resistance ($R_{total,I-V}$, Figure 4a) was estimated by calculating the slope of the current-voltage (*I-V*) curve. Results obtained previously with the electrolyte-supported AP-SOFC are also inserted for purposes of comparison. At 750°C, the total resistance decreased from 9.57 Ω cm^2 to 0.49 Ω cm^2 when the thickness of the porous CGO electrolyte was reduced from 2 mm to 112 μm. The lower resistances in anode-supported AP-SOFCs ensure higher peak power density. The total resistance of the single cell operated in C_3H_8 fuel is also shown in Figure 4a. A somewhat larger $R_{total,I-V}$ of 0.57 Ω cm^2 was obtained with C_3H_8 fuel, in agreement with previous results for classic SOFCs.[23, 24]

In order to characterise the origin of the resistances, electrochemical impedance spectroscopy measurements (EIS) were conducted. Figure 4b compares the resistance values of electrolyte-supported and anode-supported AP-SOFCs calculated from Nyquist plots. The ohmic resistance (R_{ohmic}) is derived from the high-frequency intercept on the real axis of the Nyquist plot, while the polarisation resistance (R_p) is obtained from the low-frequency (R_{LF}) intercept on the real axis minus the high-frequency (R_{HF}) intercept (R_P=R_{LF}-R_{HF}). Overall, the values of the total resistances obtained from EIS were in good agreement with those derived from the *I-V* curves (data in Figure 4a). Both single cells showed similar R_p values for anode-supported and electrolyte-supported AP-SOFCs at 750°C. The R_{ohmic} values of 0.49 Ω cm^2 and 7.19 Ω cm^2 were obtained in anode-supported and electrolyte-supported AP-SOFCs at 750°C, respectively. Clearly, the ohmic resistance of the present anode-supported AP-SOFC is greatly reduced by the thin electrolyte design. The main resistance of the cell, however, originates once again from the ohmic resistance, since 112 μm remains thick for a CGO electrolyte membrane (Figure 1). Thus, the performance of the cell might be further enhanced by obtaining a thinner electrolyte film with good porous microstructure by doping technique or using an advanced preparation method such as PLD.[25-27] Meanwhile, the polarisation resistance can also be reduced by improving the electrode structure.[28] Optimisation of the porous architecture and the cell design are beyond the scope of this study, as our aim is to demonstrate a proof of concept.

Nyquist plots of the anode-supported AP-SOFC operating with CH_4 and C_3H_8 at 600°C under OCV are shown in Figure S2. The cell showed a similar R_{ohmic} in both CH_4 and C_3H_8. The lower performances with propane are due to an increase of the R_p, as noted by Zha *et al.*[24]

Long-term operation stability and coking resistance

Long-term stability tests of the AP-SOFCs fuelled by CH_4 and C_3H_8 were carried out at 700°C under OCV conditions and then with an applied current. The results are plotted in Figure 5. It appears that the OCVs are stable in CH_4 and C_3H_8 fuels for at least around 150 h. A current of 450 mA cm^{-2} was then applied to the cell running on CH_4. A decrease of 3.2% was observed for the OCV during the period of operation, indicating that the AP-SOFCs are highly stable when CH_4 is used as fuel. This degradation could be explained by Ni coarsening at the anode.[29] The systematic study of the effect of the applied transmembrane pressure on the coking impact and electrochemical performances (OCV, Power density) goes beyond this preliminary conceptual report. Nevertheless, we anticipate that the transmembrane pressure (and consequently the oxygen flow) can be adjusted to the fuel composition and flow at the anode side in order to prevent coking.

Next, we checked whether carbon deposition had occurred in the anode. SEM analysis revealed that the tested anode maintained its highly porous structure, while no carbon was found in the Ni+CGO anode (Figure 1). Moreover, as shown in Figure S3, from the energy-dispersive X-ray spectroscopy (EDX) analysis of the anode, only negligible carbon content (<4 wt% with ~5% error in semi-quantitative analysis was

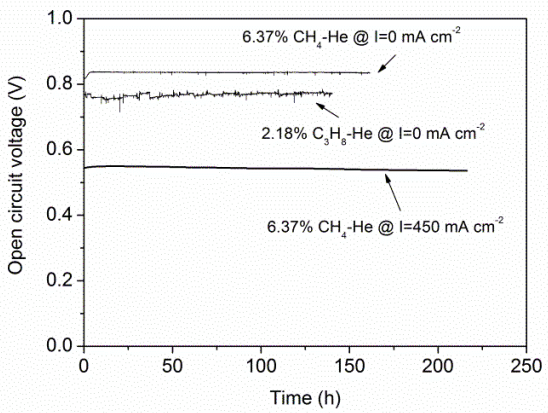

Fig. 5 Long-term stability test of the AP-SOFCs at 700°C, under OCV conditions in CH_4 and C_3H_8, and with an applied current of 450 mA cm^{-2} in CH_4.

found at the anode after the maximum duration of the cell test (220 h) in CH_4. The carbon balance is at least 98% for all experimentations which correspond to experimental analysis errors. In case of large coke formation, we should have observed a much lower value.

Conclusions

Conventional SOFCs with a Ni-based anode suffer from serious problems when operating in dry hydrocarbon fuel, due to carbon deposition. This issue could be solved efficiently and safely using an all porous SOFC (AP-SOFC) design, for which there is no need to prepare a dense electrolyte membrane. In this study, we further investigated performances and long-term stabilities of a Ni+CGO anode-supported AP-SOFC with a CGO thin-film electrolyte and BSCF+CGO cathode for CH_4-He and C_3H_8-He at intermediate temperatures. The peak power density of this anode-supported AP-SOFC reached 214 mW cm^{-2} and 179 mW cm^{-2} at 750°C with CH_4 and C_3H_8 as fuel, respectively, which was over 14 times higher than that of an electrolyte-supported AP-SOFC. The long-term stability of the AP-SOFC was tested for 220 h under a constant current of 450 mA cm^{-2} in a CH_4-He mixture at 700°C, demonstrating high stability during operation in CH_4. No visible coking or Ni coarsening was observed at the anode after operation in CH_4 for 220 h. Thus, this study demonstrates the relevance and feasibility of an all porous SOFC at the laboratory scale. We strongly believe that better performances could be achieved on a larger scale by improving cell design and by optimising the pore hierarchy of the electrolyte.

Acknowledgements

This work was supported by ADEME though the MONOPAC project. The authors thank Dr. Didier Cot and Dr. Bertrand Rebiere from Institut Européen des Membranes (Montpellier, France) for SEM and EDX analysis.

Notes and references

1. Z. P. Shao and S. M. Haile, *Nature*, 2004, **431**, 170-173.
2. J. Hanna, W. Y. Lee, Y. Shi and A. F. Ghoniem, *Progress in Energy and Combustion Science*, 2014, **40**, 74-111.
3. R. J. Gorte, H. Kim and J. M. Vohs, *Journal of Power Sources*, 2002, **106**, 10-15.
4. M. Mogensen and K. Kammer, *Annual Review of Materials Research*, 2003, **33**, 321-331.
5. X.-M. Ge, S.-H. Chan, Q.-L. Liu and Q. Sun, *Advanced Energy Materials*, 2012, **2**, 1156-1181.
6. S. P. Yoon, J. Han, S. W. Nam, T. H. Lim and S. A. Hong, *Journal of Power Sources*, 2004, **136**, 30-36.
7. Z. L. Zhan and S. A. Barnett, *Solid State Ionics*, 2005, **176**, 871-879.
8. Y. Takagi, S. Adam and S. Ramanathan, *Journal of Power Sources*, 2012, **217**, 543-553.
9. D. Mogensen, J. D. Grunwaldt, P. V. Hendriksen, K. Dam-Johansen and J. U. Nielsen, *Journal of Power Sources*, 2011, **196**, 25-38.
10. M. Yano, A. Tomita, M. Sano and T. Hibino, *Solid State Ionics*, 2007, **177**, 3351-3359.
11. M. Kuhn and T. Napporn, *Energies*, 2010, **3**, 57-134.
12. Y. Hao and D. G. Goodwin, *Journal of Power Sources*, 2008, **183**, 157-163.
13. Y. Guo, M. Bessa, S. Aguado, M. C. Steil, D. Rembelski, M. Rieu, J.-P. Viricelle, N. Benameur, C. Guizard, C. Tardivat, P. Vernoux and D. Farrusseng, *Energy & Environmental Science*, 2013, **6**, 2119-2123.
14. J. Hüppmeier, S. Barg, M. Baune, D. Koch, G. Grathwohl and J. Thöming, *Fuel*, 2010, **89**, 1257-1264.
15. Z. Chen, P. Prasad, Y. Yan and S. Elnashaie, *Fuel Processing Technology*, 2003, **83**, 235-252.
16. M. L. Rodríguez, M. N. Pedernera and D. O. Borio, *Catalysis Today*, 2012, **193**, 137-144.
17. C. Ding, H. Lin, K. Sato, K. Amezawa, T. Kawada, J. Mizusaki and T. Hashida, *Journal of Power Sources*, 2010, **195**, 5487-5492.
18. C. Xia and M. Liu, *Solid State Ionics*, 2001, **144**, 249-255.
19. C. Xia and M. Liu, *Journal of the American Ceramic Society*, 2001, **84**, 1903-1905.
20. C. Xia, F. Chen and M. Liu, *Electrochemical and Solid-State Letters*, 2001, **4**, A52-A54.
21. K. L. Duncan, K.-T. Lee and E. D. Wachsman, *Journal of Power Sources*, 2011, **196**, 2445-2451.
22. H. Yahiro, K. Eguchi and H. Arai, *Solid State Ionics*, 1989, **36**, 71-75.
23. C. Lu, W. L. Worrell, J. M. Vohs and R. J. Gorte, *Journal of The Electrochemical Society*, 2003, **150**, A1357-A1359.
24. S. Zha, A. Moore, H. Abernathy and M. Liu, *Journal of The Electrochemical Society*, 2004, **151**, A1128-A1133.
25. J. Will, A. Mitterdorfer, C. Kleinlogel, D. Perednis and L. J. Gauckler, *Solid State Ionics*, 2000, **131**, 79-96.
26. A. Tomita, S. Teranishi, M. Nagao, T. Hibino and M. Sano, *Journal of the Electrochemical Society*, 2006, **153**, A956-A960.
27. A. Infortuna, A. S. Harvey, U. P. Muecke and L. J. Gauckler, *Physical Chemistry Chemical Physics*, 2009, **11**, 3663-3670.
28. M. D. Gross, J. M. Vohs and R. J. Gorte, *Journal of Materials Chemistry*, 2007, **17**, 3071-3077.
29. G. Muller, R.-N. Vannie, A. Ringuede and C. Laberty-Robert, *The Journal of Physical Chemistry C*, 2013, **117**, 16297-16305.